Discovery and Characterization of a Novel Aryl Hydrocarbon Receptor Inhibitor, IK-175, and Its Inhibitory Activity on Tumor Immune Suppression

Karen McGovern, Alfredo C. Castro, Jill Cavanaugh, Silvia Coma, Meghan Walsh, Jeremy Tchaicha, Sakeena Syed, Prabitha Natarajan, Mark Manfredi, Xiaoyan M. Zhang, and Jeffrey Ecsedy

ABSTRACT

Aryl hydrocarbon receptor (AHR) is a transcription factor that regulates the activity of multiple innate and adaptive immune cells subsequent to binding to numerous endogenous and exogenous ligands. For example, AHR is activated by the metabolite kynurenine, which is secreted into the tumor microenvironment by cancer cells leading to broad immunosuppression. Therefore, AHR inhibition provides a novel and ideal approach to stimulate immune-mediated recognition and subsequent eradication of tumor cells. We report here the discovery and characterization of IK-175, a novel, potent and selective AHR antagonist with favorable ADME and pharmacokinetic profiles in preclinical species. IK-175 inhibits AHR activity in experimental systems derived from multiple species including mouse, rat, monkey, and humans. In human primary immune cells, IK-175 decreased AHR target gene expression and anti-inflammatory cytokine release and increased proinflammatory cytokine release. Moreover, IK-175 led to a decrease in suppressive IL17A$^-$, IL-22$^+$ expressing T cells in a Th17 differentiation assay. IK-175 dose dependently blocks ligand-stimulated AHR activation of *Cyp1a1* transcription in mouse liver and spleen, demonstrating on-target *in vivo* activity. IK-175 increases proinflammatory phenotype of the tumor microenvironment in mouse syngeneic tumors and in adjacent tumor-draining lymph nodes. As a monotherapy and combined with an anti-PD-1 antibody, IK-175 demonstrates antitumor activity in syngeneic mouse models of colorectal cancer and melanoma. IK-175 also demonstrates antitumor activity combined with liposomal doxorubicin in syngeneic mouse tumors. These studies provide rationale for targeting AHR in patients with cancer. IK-175 is being evaluated in a phase I clinical trial in patients with advanced solid tumors.

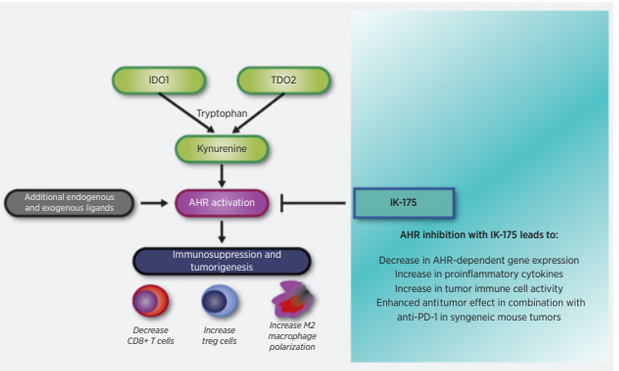

Introduction

The genetic alterations and instable genomes that enable cancer initiation and progression are accompanied by the synthesis of abnormal proteins. Fragments of these abnormal proteins (neoantigens) are presented on the surface of tumor cells via MHC-I molecules. These neoantigens can be recognized by the immune system as foreign leading to an immune response that can eradicate the neoplastic cells (1, 2). However, cancers utilize diverse mechanisms to evade immune recognition and response, enabling continued disease progression and therapeutic resistance.

One of the key mechanisms that tumors use to evade immune-mediated eradication is to secrete immunosuppressive metabolites, including kynurenine, into the tumor microenvironment. Kynurenine is synthesized from the amino acid precursor L-tryptophan by two enzymes, IDO1 and TDO2. Kynurenine binds AHR, a nuclear receptor that regulates many immune modulating genes. In addition to kynurenine, numerous endogenous and exogenous ligands are capable of binding to and activating AHR in multiple immune cells comprising both innate and adaptive immunity (3, 4). Upon binding to kynurenine or other agonists, cytoplasmic AHR is released from an inhibitory complex comprising HSP90, AHR-interacting protein (AIP) and the cochaperone p23, translocates to the nucleus, and forms a heterodimer with aryl hydrocarbon receptor nuclear translocator (ARNT; ref. 5). The AHR–ARNT complex subsequently binds to genes containing dioxin response elements (DRE) to activate gene transcription. It was also demonstrated that recognition of DNA derived from apoptotic cells by Toll-like receptor 9 can activate AHR and drive production of IL10, leading to immune tolerance (4).

Increased levels of kynurenine, IDO1 or TDO2 and activated AHR are associated with immunosuppression and correlate with poor overall prognosis in multiple cancers (6–8). Tumors expressing high levels of IDO1 have increased levels of suppressive T regulatory cells (Treg) and higher levels of immune regulatory factors including IL10, PD-L1, and CTLA4 (6). In addition, these tumors express higher levels of AHR target genes such as *CYP1B1*. This was corroborated in an analysis of TCGA data, which found a strong correlation between AHR pathway and immune suppressive markers for Treg cells, M2 myeloid cells, and inhibitory checkpoints PD-1 and CTLA4 (9). A separate

Ikena Oncology, Inc., Boston, Massachusetts.

Note: Supplementary data for this article are available at Molecular Cancer Therapeutics Online (http://mct.aacrjournals.org/).

Corresponding Author: Karen McGovern, Discovery Biology, Ikena Oncology, 645 Summer Street, Boston, MA 02210. E-mail: KMcGovern@ikenaoncology.com

Mol Cancer Ther 2022;21:1261–72

doi: 10.1158/1535-7163.MCT-21-0984

©2022 American Association for Cancer Research

Downloaded from http://aacrjournals.org/mct/article-pdf/21/8/1261/3182218/1261.pdf by guest on 23 February 2024

study of clinical patient samples revealed an enrichment of enzymes involved in kynurenine degradation in patients that benefited from anti-PD-1 treatment, supporting a link between high kynurenine levels and poor prognosis (9).

Mechanism of action studies demonstrate that AHR regulates the expression of genes that affect both the fate and functionality of multiple innate and adaptive immune cells, leading to broad immunosuppression (4, 10, 11). For example, AHR activation directs naive T cells toward a Treg fate and away from an effector T-cell fate (12, 13). We recently reported an AHR-dependent interplay between Tregs and tumor-associated macrophages driving immunosuppression in IDO1-overexpressing mouse tumors (9). In addition, AHR directly affects the differentiation and expansion of T-helper cell (Th) 22 cells and upregulates the immune suppressive cytokine IL22, a direct transcriptional target of AHR (14, 15). AHR activation can upregulate the surface inhibitory receptor PD-1 on $CD8^+$ T cells to reduce their cytotoxic activity (16). In addition, in combination with TGFβ, AHR promotes Th17 differentiation to expand Th17 cells that produce IL22 (13). Additional examples AHR's role in Th17 cells, myeloid cells such as dendritic cells (DC), and tumor macrophages have been described elsewhere (10, 13, 17).

In addition to a role for AHR in immune cells to directly prevent immune attack on cancer cells, an intrinsic role for AHR in the tumor cell has been proposed (17–19). AHR expressed in the tumor controls baseline and IFNγ-induced IDO1 and PD-L1 expression. Studies with AHR knockout (KO) mouse tumor cells led to rejection of the tumor in immune competent but not immune compromised mice (20). This rejection of AHR KO tumors after minimal growth was accompanied by a decrease in immune suppressive cells such as $CD4^+$ T cells expressing different checkpoint proteins and myeloid-derived suppressor cells and DCs expressing PD-L1 and CD39, all of which led to a greater T-cell response against the tumor.

We and others have shown that AHR-mediated immune suppression prevents immune cell attack in multiple mouse cancer models (17–19). Early AHR inhibitors have been useful for demonstrating proof of concept in nonclinical models that AHR is a viable target for overcoming immunosuppression and for driving antitumor activity in preclinical models (21–23). However, these inhibitors do not have sufficiently favorable pharmacologic properties to merit advancement into cancer clinical trials. Here, we introduce IK-175, a novel, potent, selective, and orally active inhibitor of AHR. IK-175 is currently being evaluated in a phase I clinical trial in patients with advanced solid tumors and urothelial carcinoma as a single agent and in combination with the anti-PD-1 antibody nivolumab (Clinicaltrials.gov NCT04200963).

Materials and Methods

Cell lines and primary cells

The human and rodent cancer cell lines HepG2, CT26.WT (referred to as CT26), MC38, Hepa 1.6, and H411E were obtained from ATCC; whereas authentication was not conducted, ATCC is a highly reliable cell line vendor with high standards to ensure cell line authenticity. Cynomolgus monkey peripheral blood mononuclear cells (PBMC) were obtained from HumanCells Bioscience. Cryopreserved $CD4^+$ T cells were obtained from AllCells. Cryopreserved human pan T cells and fresh leukopaks were obtained from Stemcell Technologies. HepG2 cells were cultured in RMPI1640 supplemented with 10% FBS and 2 mmol/L L-glutamine. H411E cells were maintained in EMEM supplemented with 10% heat-inactivated FBS (HI FBS). Hepa 1.6 cells were cultured in DMEM supplemented with 10% HI FBS and 1% penicillin/streptomycin. CT26 cells were maintained in RPMI1640 medium supplemented with 10% HI FBS. MC38 cells were maintained in DMEM medium with 10% HI FBS. B16-IDO1 cells were provided by the Wolchok Laboratory (Memorial Sloan Kettering Cancer Center). B16-IDO1 cells were cultured in DMEM medium supplemented with 10% HI FBS and 1 mg/mL G418 (Geneticin). Cell lines were used at passages 3 to 15, routinely screened to avoid *Mycoplasma* contamination and maintained in a humidified chamber with 5% CO_2 at 37°C. IK-175, example I-40, synthesis methods can be found in the issued U.S. patent 10,570,138 (24).

HepG2 DRE-luciferase reporter assay

HepG2 cells transiently transfected with the DRE-Luc reporter (25), were plated and dilutions of IK-175 or DMSO control and 80 nmol/L VAF347 were added in triplicate and incubated 6 hours. Media was removed and Bright Glo reagent (Promega) added to each well of the assay plate, centrifuged and incubated for 2 minutes. Luminescence was read on plate reader (Envision, with 404 mirror and 212 filter). The assay was performed >10 times with a representative sample presented here, done twice on different days ($n = 2$).

AHR binding assay

The AHR binding competition assay with human AHR protein expressed in mouse liver extracts was performed as described previously (26). Briefly, cytosol from humanized AHR mouse liver ($AHR^{Ttr}Ahr^{fx/fx}$-Cre^{alb} Line B; ref. 27) was prepared for the assay and photoaffinity ligand was made as described (26), and resuspended at a concentration of 0.21 pmol, 8×10^5 cpm/μL (saturating amount of AHR ligand) of DMSO and 1 μL of photoaffinity ligand was added to 150 μL of rat liver cytosol plus compounds IK-175 and CH223191 (both synthesized by Ikena) solutions and incubated 30 minutes at room temperature. The samples were placed on ice for 5 minutes, then 50 μL of 3% charcoal/0.3% dextran in MOPS buffer was added for 5 minutes on ice. Samples were centrifuged to remove charcoal and exposed to UV light (>302 nmol/L) for 4 minutes. Samples were run on SDS-PAGE and visualized by autoradiography. Each radioactive band was excised with a razor blade and placed in a 12 × 75 mm glass tube and counted in a gamma counter. Samples run in duplicate.

Murine Hepa1.6 and rat H411E Cyp-luciferase reporter assay

H411E or Hepa1.6 cells were plated and cultured overnight. The next day, dilutions of IK-175 and agonist (100 μmol/L kynurenine for H411E and 2 μmol/L VAF347 for Hepa1.6) were added and incubated 24 hours. Cyp1a1 enzyme activity was measured using the p450-Glo Assay (Promega) and was run according to manufacturer's instructions; luminescence was quantified on an Envision plate reader. The Hepa1.6 cells were assayed seven times, the H411E cells were assayed twice.

Cynomolgus monkey PBMCs CYP1B1 Quantigene Plex assay

Cryopreserved cynomolgus macaque PBMCs were obtained from HumanCells Bioscience and cultured in RPMI medium with 10% FBS. PBMCs, plated in 96-well round-bottom plates were treated with IK-175 ranging from 4.5 nmol/L to 10 μmol/L in duplicate in a final assay concentration of 0.1% DMSO and incubated for 24 hours at 37°C, 5% CO_2. Cells were then lysed according to the manufacturer's instructions for cultured cells (Thermo Fisher Scientific QS0100) and stored at −80°C until Quantigene Plex assay analysis.

A Quantigene Plex custom panel comprised of probes targeting primate *CYP1B1*, *AHRR*, and the housekeeping genes peptidylprolyl

Downloaded from http://aacrjournals.org/mct/article-pdf/21/8/1261/3182218/1261.pdf by guest on 23 February 2024

isomerase B (*PPIB*) and β-2 microglobulin (*B2M*) was assayed according to the manufacturer's instructions (Thermo Fisher Scientific QGP-106 Assay ID: M19050101). The mean fluorescence activity (MFI) for each gene was quantified on a Luminex FlexMap3D instrument.

Selectivity screens (receptors, transporters, and kinases)

IK-175 was screened in duplicate in the Eurofins Scientific Safety Screen 87 panel of receptors and enzymes to assess IK-175 (1 μmol/L) binding. This screen includes 13 enzyme and 74 binding assays, with reference standards. Data are presented as percent inhibition compared with controls. IK-175 was also tested in concentration response agonist and antagonist functional assays for the receptor PXR (Eurofins Scientific). IK-175 (10 μmol/L) was screened in duplicate in the Reaction Bio Kinase Panel of 371 kinases (wild-type). A subset of kinases was assayed to determine IC_{50} values: 10 doses of IK-175 with 3-fold serial dilutions starting at 10 μmol/L were used. All reactions were carried out with 10 μmol/L ATP.

In vitro cell line proliferation assays

Human cell line proliferation assays were performed on 100 cell lines at ChemPartners and murine cell lines tested at Ikena. Briefly, human cells were treated with nine concentrations of IK-175 ranging from 1 nmol/L to 10 μmol/L and mouse cells treated with six concentrations of IK-175 ranging from 33 nmol/L to 10 μmol/L and incubated for 3 days at 37°C. Cell viability was measured using Cell Titre Glo (Promega).

Human Pan-T-cell activation and RNA prep for qRT-PCR and cytokine analysis

Cryopreserved pan-T cells were activated with human CD3/CD28 T-cell activator (12.5 μL/1 × 10^6 cells, Stemcell Technologies) and added to a 96-well plate in T-cell medium (RPMI1640 + 10% HI FBS, 1× penicillin/streptomycin, 2 mmol/L L-glutamine, 0.1 mmol/L non-essential amino acids, 1 mmol/L sodium pyruvate, 10 mmol/L HEPES, 55 μmol/L β-mercaptoethanol) at 50,000 cells/well. Cells were treated with DMSO and different concentrations of KYN-101 (9) or IK-175 in duplicate.

qRT-PCR

After 24 hours, cDNA was collected using Cells-to-CT Kit (Thermo Fisher Scientific). The RT-PCR reaction was conducted using Taqman fast advanced master mix (Thermo Fisher Scientific), human *CYP1A1* primer (Hs05011273_s1, Thermo Fisher Scientific), or human *IL22* primer (Hs01574154_m1, Thermo Fisher Scientific) and *B2M* housekeeping gene (Hs00187842_m1, Thermo Fisher Scientific) and was run in the QuantStudio Real-Time PCR System. The experiment was repeated with T cells from three different donors.

Cytokine analysis

Activated human T cells were treated with IK-175 for 48 hours, then supernatant was analyzed for levels of secreted cytokine IL22 and IL2 using off-the-shelf V-plex IL22 and IL2 plates [meso scale discovery (MSD)]. The MSD assay was performed according to manufacturer's instructions and analyzed using MSD software. IC_{50} values for inhibition of IL22 production were calculated using the GraphPad Prism algorithm for nonlinear four parameter curve regression.

Human Th17 differentiation assay

Naive human T cells ($CD4^+$/$CD62L^+$) from two independent donors were isolated from cryopreserved $CD4^+$ T cells (AllCells) by magnetic selection with human CD62 L microbeads (Miltenyi). On Day 1, naive $CD62L^+$ human T cells were activated with human CD3/CD28 T-cell activator (12.5 μL/1 × 10^6 cells, Stem Cell Technologies) and differentiated with human Th17 cytokines (50 ng/mL IL6, 20 ng/mL IL1β, 10 ng/mL IL23, 1 ng/mL TGFβ, 12 μg/mL antihuman IFNγ antibody, and 10 μg/mL antihuman IL4 antibody; Peprotech) for 11 days. Concurrently, cells were treated with DMSO, 3 μmol/L IK-175, or 3 μmol/L ITE. All conditions were in biological triplicate. Media containing cytokine cocktail, CD3/CD28 and the above compounds was refreshed every 2 to 3 days.

On Day 11, cells were stimulated with 1× Cell Stimulation Cocktail (PMA and Ionomycin; eBioscience) for 5 hours and then cells were stained for intracellular cytokines (human CD4, IL17A, IL22; BioLegend). Samples were run on a BD LSR Fortessa flow cytometer and analyzed in FlowJo software (BD Biosciences).

Animals

Mice were housed in groups of five in suspended, stainless-steel cages. Food (Rodent lab chow) and water (autoclaved filtered tap water in bottles) were provided ad libitum. Cages were changed every 10 to 14 days during the study. The animal facility maintained a 12-hour light/12-hour dark cycle with manual override, 30% to 70% humidity, and temperature range of 65 to 78°F (18–26°C). All protocols were approved by, and all experiments were conducted in accordance with the Institutional Animal Care and Use Committee.

For *in vivo* tumor studies, 6- to 8-week-old, female C57BL/6 and Balb/c mice were obtained from The Jackson Laboratories. Upon delivery, all animals underwent at least 72 hours of acclimatization before handling.

Pharmacokinetics

The mouse pharmacokinetics study was performed at WuXiAppTec. Rat and cynomolgus monkey pharmacokinetics studies were performed at Covance; the dog pharmacokinetics study was performed at PCRS and analyzed at Seventh Wave. Female Balb/c mice were administered 3 mg/kg IK-175 either intravenously or orally. Male Sprague–Dawley rats were administered IK-175 at 2.5 mg/kg intravenously and 5 and 25 mg/kg orally. Male beagle dogs were administered IK-175 at 0.5 mg/kg intravenously and 2.5 mg/kg orally. Male cynomolgus monkeys were administered 2.5 mg/kg IK-175 intravenously and 5 and 25 mg/kg orally. The intravenous formulation for all species was 5% DMSO, 75% PEG400, 20% water; this formulation was also used for the dog oral formulation. The mouse oral formulation was 30% PEG 400, 10% Solutol, 60% water; the rat oral formulation was 100% Labrafil M1944 CS; the monkey oral formulation was 10% Solutol, 5% Tween 80 in water. Blood was collected in a standard time course and plasma levels of IK-175 were measured by LC/MS.

Cyp1b1, Ido1, and IFNγ qRT-PCR in mice

RNA was extracted from tumor samples (~100 mg each) with the RNEasy Mini RNA Extraction Kit (Qiagen) according to the manufacturer's instructions. RNA concentration and purity were measured by Nanodrop and reverse transcribed with Superscript IV VILO master mix (Thermo Fisher Scientific) according to the manufacturer's instructions.

Expression of the mouse Cyp1b1 (Mm00487229_m1), *Ido1* (Mm00492586_m1), *Ifnγ* (Mm01168134_m1), and the housekeeping gene *Hprt1* (Mm03024075_m1) were quantified by qPCR using the TaqMan Fast Advanced Gene Expression Master Mix and TaqMan probes (Thermo Fisher Scientific).

Downloaded from http://aacrjournals.org/mct/article-pdf/21/8/1261/3182218/1261.pdf by guest on 23 February 2024

Ex vivo tumor draining lymph node (TDLN) stimulation and tumor immunophenotyping

CT26 cells (5×10^5 cells, in sterile PBS) were implanted subcutaneously in the right flank of each Balb/c mouse. Seven days postimplant, mice were randomized into treatment groups by tumor volume (average 100 mm^3) and body weight. IK-175 (in 0.5% MC in sterile water) and administered at 25 mg/kg by oral gavage, once daily. After seven days of treatment, the TDLNs were mechanically homogenized through a 70 μmol/L nylon cell strainer, washed two times with PBS and 1×10^6 cells per well were plated with or without 1× Cell Stimulation Cocktail (PMA and Ionomycin; eBioscience) and 1× Protein Transport Inhibitor Cocktail (eBioscience). After 5 hours, cells were washed and resuspended in FACS buffer (2% HI FBS in PBS) and stained for 30 minutes at room temperature with surface and intracellular antibodies (BioLegend): CD45 (30-F11, 1:200), CD3 (17A2, 1:200), CD4 (RM4–5, 1:200), CD8 (53–6.7, 1:200), IL2 (JES6–5H4, 1:200), IFNγ (2E2, 1:300), TNFα (1:200), and Fixable Live/Dead Aqua (Thermo Fisher Scientific, 1:1,000). Samples were run on a BD LSR Fortessa flow cytometer and analyzed with FlowJo software (BD Biosciences).

Tumors were mechanically homogenized with scissors, dissociated with Mouse Tumor Dissociation Kit (Miltenyi) and strained through a 70 μmol/L nylon cell strainer. Cells were washed two times with PBS and 1×10^6 cells per well were stained for 30 minutes at room temperature with surface and intracellular antibodies (BioLegend): CD45 (30-F11, 1:200), CD11b (M1/70, 1:300), F4/80 (BM8, 1:200), Ly6G (1A8, 1:200), CD11c (N418, 1:100), Ly6C (AL-21, 1:200), CD206 (C068C2, 1:200), and MHCII (M5/114.15.2, 1:300) and Fixable Live/Dead Aqua (Thermo Fisher Scientific, 1:1,000). Samples were run on a BD LSR Fortessa flow cytometer and analyzed with FlowJo software (BD Biosciences).

In vivo tumor efficacy with anti-PD-1 antibody

B16-IDO1 efficacy

B16-IDO1 cells (2×10^5 in sterile PBS) were implanted intradermally in each C57BL/6 mouse. Seven days postimplant, mice were randomized into treatment groups by tumor volume (average 30 mm^3) and body weight. Regimen for single agents or combination treatments: inhibitor IK-175 was dissolved in 0.5% methyl cellulose (MC) in sterile water and administered at 25 mg/kg by oral gavage, once daily, anti-PD-1 antibody (10 mg/kg), clone RPM1–14, Bio X cell) or rat IgG (10 mg/kg, clone 2A3, BioXcell) was injected intraperitoneally every 3 days for five doses, starting from Day 7 after tumor implantation.

CT26 efficacy

CT26 (5×10^5 cells in sterile PBS) were implanted subcutaneously in the right flank of each Balb/c mouse. Four days postimplant, mice were randomized into treatment groups by tumor volume (average 40 mm^3) and body weight. Regimen for single agents or combination treatment: AHR inhibitor IK-175 was dissolved in 0.5% MC in sterile water and administered at 25 mg/kg by oral gavage, once daily. Anti-PD-1 antibody (10 mg/kg, clone RPM1–14, BioXcell) or Rat IgG (10 mg/kg, clone 2A3, BioXcell) was injected intraperitoneally twice weekly for five doses, starting from day 4 after tumor implantation.

In vivo tumor efficacy with liposomal doxorubicin

CT26 efficacy

CT26 cells (5×10^5 cells in sterile PBS) were implanted subcutaneously in the right flank of each Balb/c mouse (100 total). Four days postimplant, 50 mice with palpable tumors were dosed intravenously with 1 mg/kg liposomal doxorubicin (Doxil; Blue Door Pharma). Seven days postimplant, the 50 liposomal doxorubicin-treated mice were randomized by tumor volume and body weight into liposomal doxorubicin alone or IK-175 + liposomal doxorubicin treatment groups. The remaining untreated mice were randomized by tumor volume (average 70 mm^3) and body weight into vehicle or IK-175 treatment groups. Beginning on Day 7 postimplant, IK-175 was given as a single agent or in combinations with liposomal doxorubicin. IK-175 was dissolved in 0.5% MC in sterile water and administered at 25 mg/kg by oral gavage, once daily. Liposomal doxorubicin was administered at 1 mg/kg (5 mL/kg in sterile saline) intravenously, once weekly.

MC38 efficacy

MC38 cells (1×10^6 in sterile PBS) were implanted subcutaneously in the right flank of each C57BL/6 mouse. Six days postimplant, mice were randomized into treatment groups by tumor volume (average 90 mm^3) and body weight. Treatments were given as single agents or in combinations with the following regimen for each drug. IK-175 was dissolved in 0.5% MC in sterile water and administered at 25 mg/kg by oral gavage, once daily. Liposomal doxorubicin was administered at 0.25 mg/kg (5 mL/kg in sterile saline) intravenously, once weekly. Treatment started 6 days post-cell inoculation.

For all studies, tumors were measured three times per week with a caliper, and the tumor size was calculated with the following equation: $(L \times W \times W)/2$. Mice that had no visible or palpable tumors that could be measured on three consecutive measurement days were considered complete regressions. Body weight was measured three times per week. Animals were euthanized when the tumor volume exceeded 2,000 mm^3.

Statistical analysis

In vivo data are presented as mean ± SEM and statistical analysis was performed using GraphPad Prism V8 software. An unpaired *t* test or Student *t* test was used as indicated to determine the *P* value and *P* values were considered significant below 0.05 (*, $P \le 0.05$; **, $P \le 0.01$; ***, $P \le 0.001$).

Data availability statement

The data generated in this study are available upon request from the corresponding author.

Results

Discovery and characterization of IK-175: a novel, selective inhibitor of AHR

Lead optimization studies starting from reported AHR inhibitor SR-1 led to the identification of IK-175, a novel, potent AHR inhibitor with favorable pharmacological properties (**Fig. 1A**). In human HepG2 cells expressing an AHR-dependent DRE-luciferase reporter and stimulated with 80 nmol/L of the AHR agonist VAF347 (28), IK-175 inhibited luciferase expression with an IC_{50} of 91 nmol/L (**Fig. 1B**). Inhibition of the DRE-luciferase with IK-175 was also assessed after addition of other AHR agonists including kynurenine (200 μmol/L), kynurenic acid (200 μmol/L), and 2-(1′H-indole-3′carbonyl)-thiazole-4-carboxylic acid methyl ester (ITE, 20 nmol/L), and IC_{50} values of 89, 30, and 68 nmol/L were observed, respectively (**Table 1**). It has been demonstrated that certain compounds that bind AHR can have both agonistic and antagonistic activity (29). IK-175 was tested in the HepG2 DRE-luciferase reporter assay without addition of exogenous ligand and there was no activation of AHR with IK-175, indicating that IK-175

Downloaded from http://aacrjournals.org/mct/article-pdf/21/8/1261/3182218/1261.pdf by guest on 23 February 2024

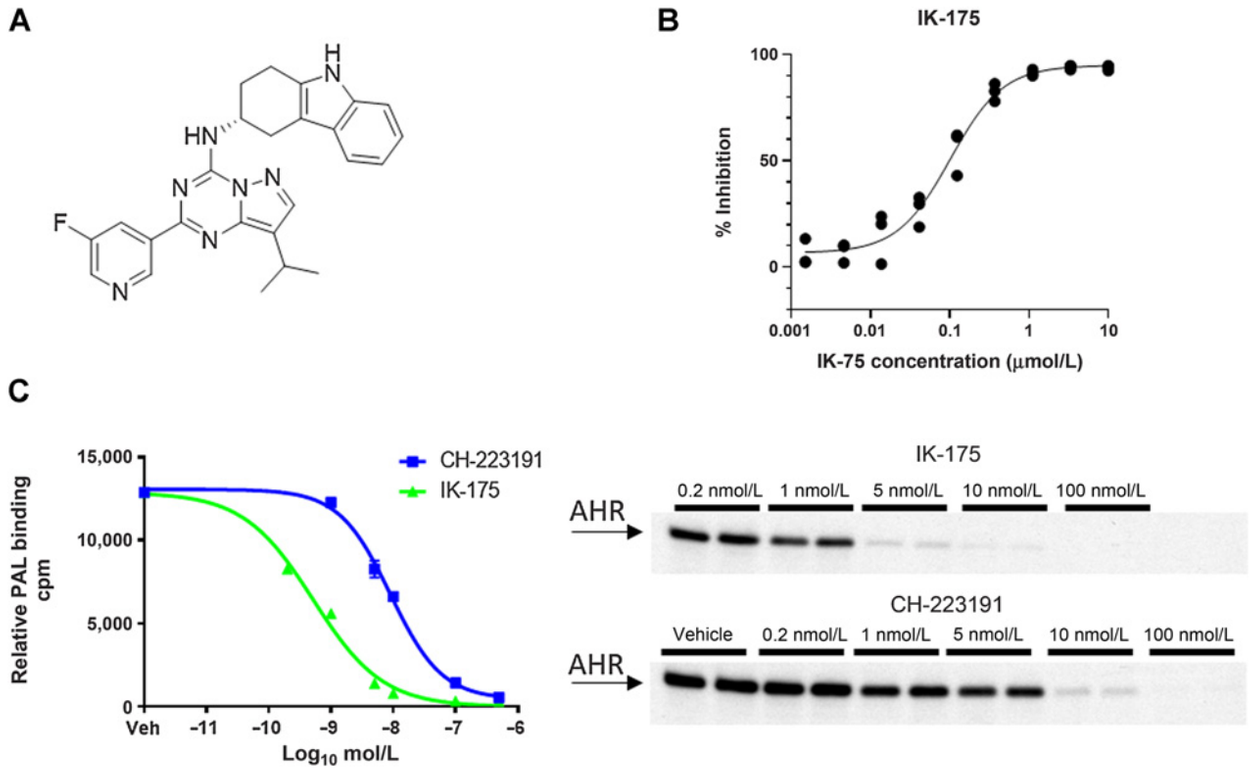

Figure 1.

A, Structure of IK-175. **B,** Activity of IK-175 in HepG2 DRE-Luc reporter assay (done in triplicate). **C,** AHR radioligand binding competition assay, quantitation of autoradiography (left) and autoradiography of SDS-PAGE (right) affinity curve (right; $n = 1$, performed in duplicate).

does not have agonist activity in this assay. In fact, IK-175 inhibited the basal activity in these cells with an IC_{50} of 14 nmol/L (Supplementary Fig. S1).

IK-175 directly binds to AHR with high affinity

The ability of IK-175 to directly bind AHR and displace a ligand was evaluated in a photoaffinity ligand competition assay (26, 27). Liver cytosol was prepared from humanized AHR mice ($AHR^{Ttr}Ahr^{fx/fx}$-Cre^{alb}), which have the murine AHR removed via the Cre recombinase, Ahr-floxed conditional knockout and instead express human AHR under the control of the liver-specific transthyretin promoter (27). This humanized AHR liver cytosol was treated with a radiolabeled dioxin analog (2-azido, 3 iodo[^{125}I], 7,8-dibromo-dibenzo-*p*-dioxin) and increasing concentrations IK-175 or a tool AHR inhibitor CH-223191 (30). Ligand displacement was measured by running lysates on SDS-PAGE, followed by autoradiography. IK-175 displaced the dioxin analog on AHR with an IC_{50} of 0.5 nmol/L, whereas CH-223191 had an IC_{50} of 9.0 nmol/L (**Fig. 1C**).

IK-175 disrupts AHR-dependent transcription in multiple species

The ability of IK-175 to inhibit AHR in nonhuman species was also evaluated in the mouse Hepa1.6 cell line using a luciferase assay that measures cytochrome P450 enzyme Cyp1a1 activity whose expression is driven by AHR. As with the human hepatocellular cell line HepG2, Hepa1.6 cells express high levels of AHR. The Hepa1.6 cells were treated with 2 μmol/L of the AHR agonist VAF347 and a concentration range of IK-175. Inhibition of activated AHR by IK-175 was indirectly assessed by decrease in Cyp1a1-mediated luciferase activity and had an IC_{50} of 36 nmol/L (**Table 1**; Supplementary Fig. S2A). IK-175 also inhibited AHR activity with an IC_{50} of 151 nmol/L in the rat hepatoma cell line H411E using the same Cyp1a1 activity assay and activated with

Table 1. Cellular activity of IK-175.

	Human HepG2				Murine Hepa1.6	Rat H411E	Cynomolgus monkey PBMCs
Assay	DRE-Luc reporter				Cyp-Luc assay		Cyp1b1 qRT-PCR
Agonist	VAF347 (80 nm)	Kynureine (200 μmol/L)	Kynurenic acid (200 μmol/L)	ITE (20 nmol/L)	VAF347 (2 μmol/L)	Kynurenine (100 μmol/L)	NA
EC_{50}	91 nmol/L	89 nmol/L	30 nmol/L	68 nmol/L	36 nmol/L	151 nmol/L	6.2 nmol/L

Downloaded from http://aacrjournals.org/mct/article-pdf/21/8/1261/3182218/1261.pdf by guest on 23 February 2024

100 μmol/L kynurenine (**Table 1**; Supplementary Fig. S2B). In cynomolgus monkey, PBMCs IK-175 inhibited expression of the AHR-dependent gene *CYP1B1* with an IC_{50} of 6.2 nmol/L (**Table 1**; Supplementary Fig. S2C). There is no indication of activation of AHR, supporting the activity of IK-175 as an AHR antagonist with no agonist activity in these assays.

IK-175 is a selective AHR inhibitor

IK-175 was evaluated in multiple assays to assess its selectivity for AHR. IK-175 showed limited activity against a panel of 87 receptors, transporters, and enzymes when screened at 1 μmol/L (Supplementary Table S1). The potential for agonist and antagonist activity of IK-175 against pregnane X receptor (PXR), a receptor structurally similar to AHR, was also assessed. IK-175 did not demonstrate agonistic activity against PXR and only minimal inhibitory activity at concentrations above 3 μmol/L (Supplementary Fig. S3). In a screen of 371 kinases, 10 μmol/L IK-175 inhibited only six kinases with inhibitory activity levels >65%. These six kinases, CDK2/cyclin E, CDK2/cyclin E2, CHK2, CK1d, DAPK1, and SRPK2, were assayed with decreasing concentrations of IK-175 and the resulting IC_{50} values ranged between approximately 2 and 9 μmol/L (Supplementary Table S2).

IK-175 has no direct effect on human or murine cancer cell lines

IK-175 was tested in concentration response assays for growth inhibition effects on 100 human cancer cell lines and no growth inhibition was detected (Supplementary Table S3). IK-175 also had no anti-proliferative effects in the murine cancer cell lines CT26 and B16-IDO (Supplementary Fig. S4).

IK-175 inhibits AHR-dependent transcription and plays a role in human T-cell fate

We have previously shown that AHR inhibition with a related AHR inhibitor KYN-101 affects the profile of cytokines produced by activated T cells derived from human donors. In particular, AHR inhibition decreased IL22 and increased IL2 in multiple donors (Supplementary Fig. S5). The activity of IK-175 was assessed in a concentration response in activated human T cells by examining the effects on AHR-dependent gene expression and cytokine production. Treatment of $CD3^+$/$CD28^+$ activated human T cells with IK-175 inhibited *CYP1A1* and *IL22* gene expression in a concentration-dependent manner with IC_{50} values of 11 and 30 nmol/L, respectively (**Fig. 2A**). MSD analysis of cytokines produced by T cells demonstrated that IK-175 inhibits IL22 production with an IC_{50} of 7 nmol/L (**Fig. 2B**) and increases proinflammatory IL2 cytokine production 2-fold (**Fig. 2B**). We previously demonstrated that the effect of kynurenine increased Treg suppressive activity but Treg cells from AHR KO mice had diminished inhibitory function over T-cell activation (9). These data indicate that AHR inhibition with IK-175 has a direct effect on T cells and can shift T cells to a more proinflammatory phenotype.

AHR has been reported to play a role in Th17 cell differentiation (13). The activity of IK-175 in a Th17 differentiation assay was evaluated by flow cytometry; ITE, an AHR agonist, was added as a control. AHR inhibition with IK-175 led to an increase in $IL17A^+$, $IL22^-$ expressing cells and a decrease in $IL17A^-$, $IL22^+$ expressing cells (**Fig. 2C**; refs. 13, 14). The reverse was found with the AHR agonist ITE which led to an increase in $IL22^+$ expressing cells. These data demonstrate that IK-175 can constrain the formation of immune suppressive T cells.

Pharmacokinetic properties of IK-175 in multiple species and on-target AHR activity in mice

The pharmacokinetics of IK-175 in Balb/c mice were assessed after intravenous and oral administration of a single 3 mg/kg dose (**Fig. 3A**). IK-175 exposure with intravenous versus oral dosing determined that the oral bioavailability for was approximately 50% with an elimination half-life of approximately 7 hours. Therefore, IK-175 is orally bioavailable with acceptable pharmacokinetic properties for murine studies. The pharmacokinetics of IK-175 were also evaluated in Sprague–Dawley rats, beagle dogs, and cynomolgus monkeys (Supplementary Figs. S6A–S6C). IK-175 displayed good oral exposure over 24 hours in rats (Supplementary Fig. S6A) and cynomolgus monkeys (Supplementary Fig S6C). There was lower exposure in dogs that was likely due to the fact the dogs had mild emesis immediately following the oral dose, which also occurred in vehicle treated animals and was therefore likely due to the oral formulation (Supplementary Fig S6B). These data supported the selection of rats and cynomolgus monkeys for subsequent nonclinical studies with IK-175.

AHR inhibition *in vivo* was evaluated in a murine pharmacodynamic study by measuring AHR dependent gene expression in the liver and spleen. Mice were treated with VAG539 (30 mg/kg, orally), a prodrug of VAF347, to activate AHR concurrently with vehicle or IK-175 (5, 10, or 25 mg/kg). *Cyp1a1* RNA expression was measured via qRT-PCR in livers and spleens at 4 and 10 hours after dosing. Four hours after VAG539 treatment alone, *Cyp1a1* levels were induced by approximately 900- and 13-fold in the liver and spleen, respectively (**Fig. 3B** and **C**). Lower *Cyp1a1* expression at 10 hours than 4 hours was likely due to the short half-life of VAF347, which is <25 ng/mL in mouse plasma 12 hours post-dose of VAG539 (Supplementary Fig. S7). IK-175 inhibited AHR dependent expression of *Cyp1a1* in both a time- and dose-dependent manner in liver and spleen (**Fig. 3B** and **C**). The level of inhibition in the liver at 4 hours was 78%, 93%, and 98% for 5, 10, and 25 mg/kg, respectively, with 25 mg/kg maintaining full inhibition (> 94%) at 10 hours. In the spleen, the level of inhibition at 4 hours was 35%, 76%, and 97% for 5, 10, and 25 mg/kg, respectively. These data indicate that IK-175 can potently inhibit AHR in vivo. Given that the pharmacodynamic effect of IK-175 in liver and spleen saturated at a dose of 25 mg/kg, the majority of in vivo antitumor efficacy studies used a high dose of 25 mg/kg.

IK-175 treatment alters the immune microenvironment in TDLNs and tumors to a proinflammatory environment

We previously demonstrated that AHR inhibition using small molecules leads to multiple changes in immune cells resulting in a more proinflammatory tumor microenvironment (9). The effect of IK-175 on immune cells within tumor-draining lymph nodes (TDLNs) was evaluated here in mice bearing syngeneic colon cancer CT26 tumors. Seven days after mice were inoculated with CT26 tumor cells, IK-175 (25 mg/kg) was administered daily for seven days. TDLNs were analyzed by flow cytometry for $CD8^+$ T cells and expression of proinflammatory cytokines upon ex vivo stimulation with PMA/ionomycin. IK-175 treatment led to higher levels of $CD8^+$ T cells in the TDLNs (Supplementary Fig. S8A) and these $CD8^+$ T cells produced higher levels of IL-2, TNFα, and IFNγ (Supplementary Fig. S8B, which suggests that IK-175 led to more proinflammatory T cells. Analysis of the T cell populations in unstimulated samples showed that while the change in absolute numbers of the $CD8^+$ and Treg (CD4+/FoxP3+/CD25+) cells in TDLNs between vehicle and IK-175 treated animals did not reach statistical significance ($p < 0.05$), the $CD8^+$:Treg ratio did reach statistical significance (Supplementary Fig. S8C). We previously showed that AHR inhibition affects the tumor immune cell

Downloaded from http://aacrjournals.org/mct/article-pdf/21/8/1261/3182218/1261.pdf by guest on 23 February 2024

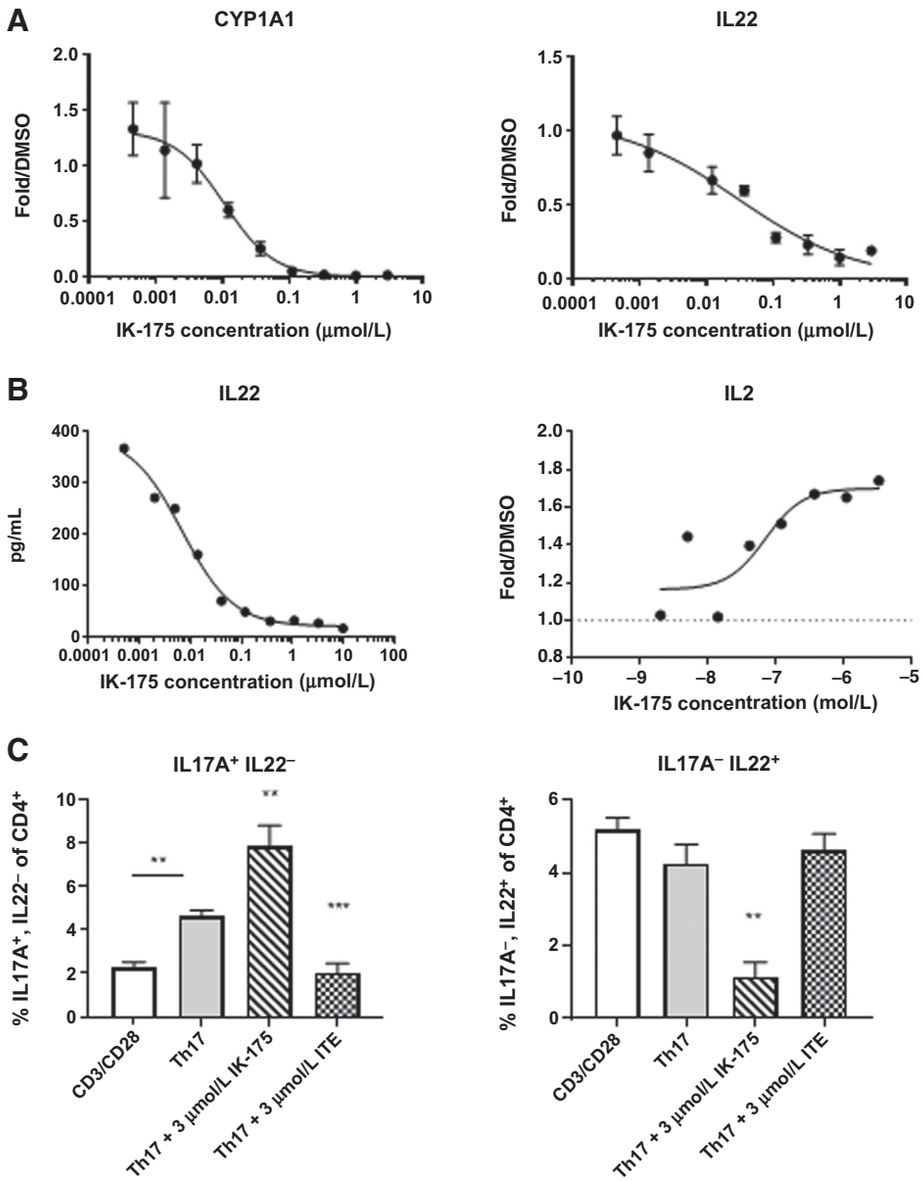

Figure 2.

Activity of IK-175 in human T cells. **A,** Inhibition of CYP1A1 and IL22 gene expression in activated T cells. **B,** Inhibition of IL22 and IL2 cytokine production in activated T cells. **C,** Increase in IL17A$^+$ (left) and decrease in IL22$^+$ (right) human T cells under Th17 polarizing conditions (significance compared with Th17 alone: $^{**}P < 0.01$, $^{***}P < 0.001$, unpaired *t* test). Data are from one representative donor performed in triplicate.

infiltrate leading to a shift from an immune suppressive to an inflammatory tumor microenvironment, including a decrease in regulatory T cells and myelosuppressive cells in the B16 mouse model overexpressing IDO1 (9). Treatment with IK-175 led to a similar shift in the immune cell composition in the CT26 tumor model, increasing the proinflammatory myeloid M1 (MHCII$^+$ CD206$^-$) subtype to shift the overall M1:M2 ratio (Supplementary Fig. S8D, gating strategy Supplementary Fig S9).

IK-175 inhibits tumor growth as a single agent and in combination with the immune checkpoint inhibitor anti-PD-1

B16-IDO1 tumors were first developed to better understand the role of IDO in tumor immune suppression (30). The B16-IDO1 model overexpresses IDO1 leading to high kynurenine production, and subsequently, a more immune suppressive tumor microenvironment and more aggressive growth (9, 31). Given the importance of AHR as the receptor for kynurenine, in vivo efficacy studies were performed with IK-175 in the B16-IDO1 syngeneic tumor model to evaluate its effects as a single agent and in combination with anti-PD-1 checkpoint inhibitor. B16-IDO1 cells were implanted intradermally in mice and treatment was initiated after measurable tumors were established. IK-175 and the anti-PD-1 antibody inhibited tumor growth when each were administered as single agents relative to vehicle treated animals, although tumor growth inhibition with IK-175 alone was not statistically significant (**Fig. 4A** and **B**). IK-175 in combination with anti-PD-1 had a significantly increased antitumor effect compared with either single agent alone, including one complete response (CR). There was no body weight loss over the course of the study.

IK-175 alone and in combination with anti-PD-1 was also evaluated in a syngeneic colon carcinoma tumor CT26 model, since CT26 tumors express high levels of IDO1 endogenously. Again, IK-175 and anti-PD-1 were administered as single agents and in combination in

Downloaded from http://aacrjournals.org/mct/article-pdf/21/8/1261/3182218/1261.pdf by guest on 23 February 2024

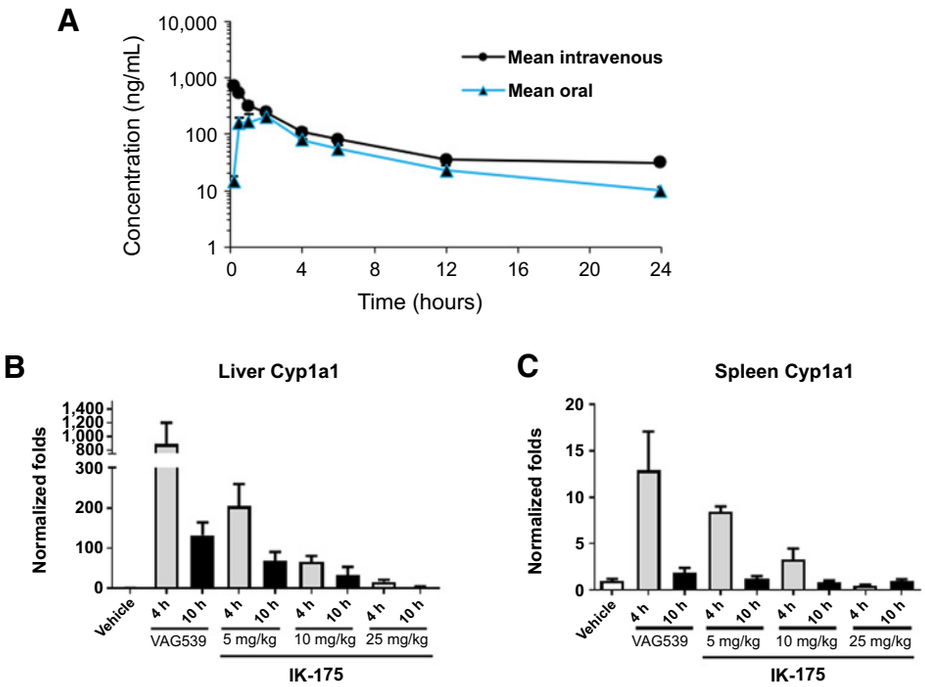

Figure 3.
Pharmacokinetics and pharmacodynamics of IK-175 in mice. **A,** Time course of plasma exposure after intravenous and oral dosing of IK-175 (3 mg/kg) in Balb/c mice; AUC for intravenous and oral dosing is 2,081 and 1,091 ng × h/mL, respectively, with a C_{max} of 204 ng/mL with oral dosing. **B** and **C,** AHR inhibition *in vivo* as measured by Cyp1a1 gene expression, with treatment of IK-175 (5, 10, and 25 mg/kg) along with agonist VAG539 for 4 or 10 hours, in **B**, liver and **C**, spleen.

established tumors. There was significant tumor growth inhibition with IK-175 as a single agent and in combination with anti-PD-1 (**Fig. 4C**). In addition, there were seven CRs in the combination group, compared with four CRs in the anti-PD-1 group (**Fig. 4D**); this led to enhanced survival in the combination group (**Fig. 4E**). There was no body weight loss over the course of the study. Mice with a CR were rechallenged with CT26 cells 90 days after CR was confirmed. None of the mice with CRs developed tumors while all the naive mice implanted with the same CT26 cells had tumors of >2,000 mm^3 by 22 days (Supplementary Fig. S10). The lack of tumors in mice that were rechallenged with CT26 cells supports the hypothesis that the anti-tumor activity was mediated by an immune mechanism. These data support previous reports that AHR inhibition shifts the tumor microenvironment from an immune suppressive to a more inflammatory environment. Inhibition of AHR with IK-175 inhibits tumor growth as a single agent, complements the activity of anti-PD-1, and provides rationale for this combination in patients with cancer.

IK-175 displays enhanced tumor growth inhibition in combination with liposomal doxorubicin

It has been reported that liposomal doxorubicin can stimulate immunogenic cell death (32). To determine if liposomal doxorubicin influences AHR activation, CT26 tumor-bearing mice were treated with 5 mg/kg liposomal doxorubicin on Day 1 and Day 7 and tumor gene expression was analyzed one day after the second dose. Liposomal doxorubicin treatment led to increased AHR pathway activation, as measured by *Cyp1b1* and *Ido1* expression, and increased *Ifnγ* gene expression that can also lead to higher *Ido1* (Supplementary Fig. S11). To determine the effect on tumor growth, IK-175 and liposomal doxorubicin were combined in various syngeneic models. CT26 tumors were established and treated with liposomal doxorubicin and IK-175 as described in methods. While IK-175 had a modest effect on the larger CT26 tumors, combination with liposomal doxorubicin lead to significant tumor growth inhibition compared with liposomal doxorubicin alone (**Fig. 5A** and **B**). There was also one CR in the combination group and enhanced survival (**Fig. 5C**). There was no body weight loss over the course of the study (**Fig. 5D**). The combination with IK-175 and liposomal doxorubicin was also examined in the syngeneic colon cancer model MC38. Combination activity was again demonstrated by significant tumor growth inhibition with the two agents compared with either alone (Supplementary Fig. S12). These data suggest that AHR inhibition may combine well with agents that induce AHR activity and/or immunogenic cell death.

Discussion

We identified and characterized a novel, potent AHR inhibitor, IK-175, with good pharmaceutical properties for clinical development. While multiple studies demonstrated a role for AHR in tumor immune suppression, these studies used either AHR KO cell lines or suboptimal tool compounds that are not amenable to evaluation in human clinical trials. IK-175 is a highly selective potent AHR inhibitor with PK properties that permit daily oral dosing with good bioavailability in rat and cynomolgus monkeys, species selected for additional non-clinical studies. The oral bioavailability was lower in the dog studies, likely due to emesis that occurred in dogs orally dosed with either vehicle or IK-175. IK-175 inhibits the ability of multiple AHR agonists to activate AHR and demonstrates activity in mouse, rat, cynomolgus monkey, and human cell systems. IK-175 demonstrates an effect on human T cells in vitro, with direct effects on gene expression and cytokines IL-22 and IL-2. In the cell line assays and in T cell assays, IK-175 inhibited AHR with no activation that would suggest that it has no activity as an AHR agonist. AHR inhibition during Th17 differentiation decreases immune suppressive IL-22^+, IL-17^- expressing cells. IK-175 treatment of tumor-bearing mice alters T cells and myeloid cells in murine tumors and TDLNs. In a previous study, the AHR agonist kynurenine increased Treg suppressive activity, but Treg cells from AHR knockout mice had diminished inhibitory function over T cell activation (9). In vivo studies here show a decrease in Treg cells, with a slight increase in $CD8^+$ cells leading to an increase in $CD8^+$:Treg ratio, and an

Downloaded from http://aacrjournals.org/mct/article-pdf/21/8/1261/3182218/1261.pdf by guest on 23 February 2024

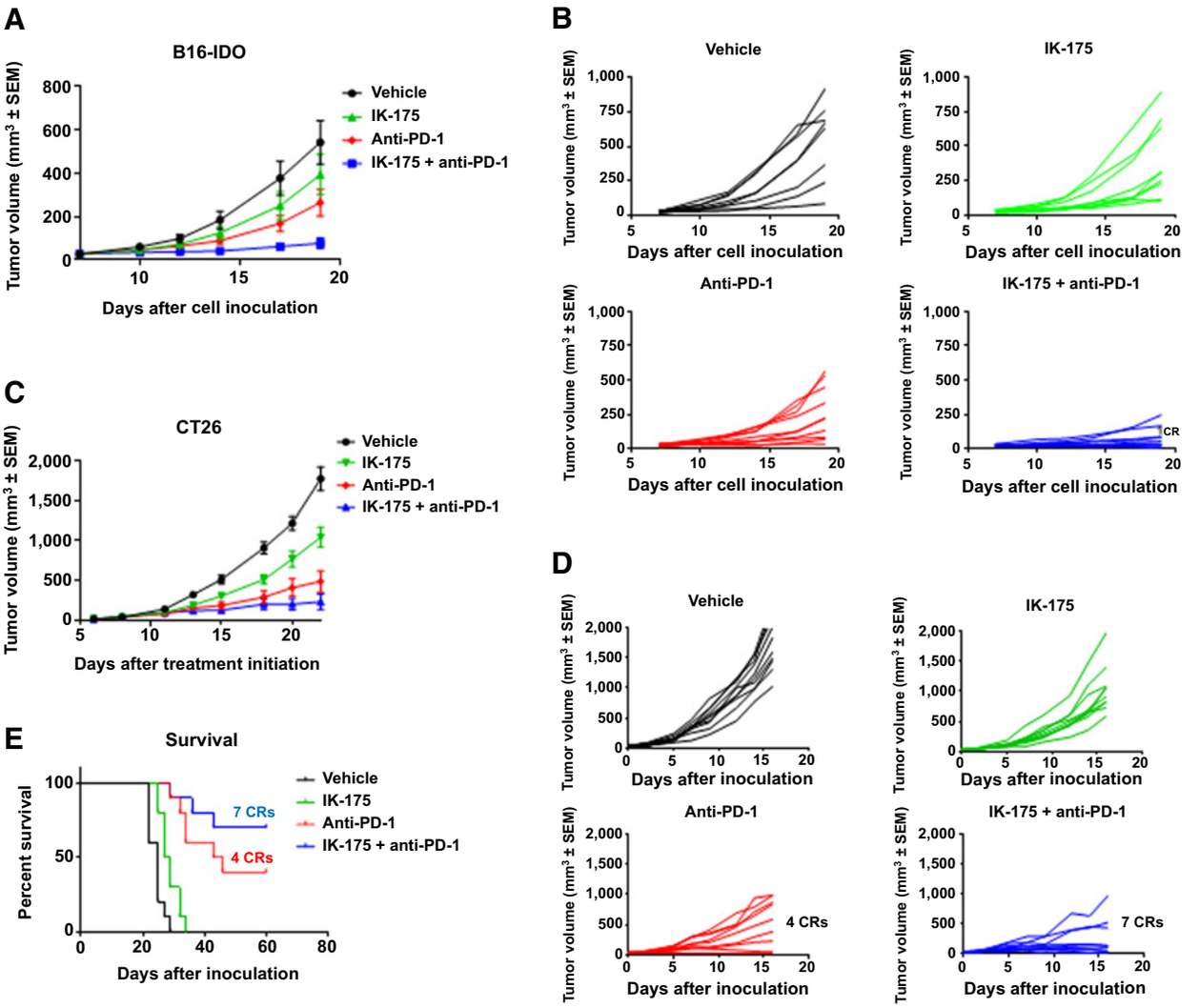

Figure 4.

Activity of IK-175 as a single agent and in combination with anti-PD-1 on B16-IDO1 and CT26 tumor growth. IK-175 at 25 mg/kg, orally, every day; anti-PD-1 at 10 mg/kg, i.p., every 3 days for five doses. **A,** Tumor growth over time in B16-IDO1 (anti-PD-1 vs. vehicle $P = 0.025$; IK-175 and anti-PD-1 vs. vehicle $P = 0.0001$; IK-175 and anti-PD1 vs. anti-PD-1, $P = 0.01$; IK-175 single agent, TGI not significant; unpaired t test). Treatment started 7 days post-inoculation. **B,** Individual tumors by group. **C,** Tumor growth over time in CT26 (IK-175 vs. vehicle, $P = 0.0015$; anti-PD-1 vs. vehicle, $P < 0.0001$; IK-175 plus anti-PD-1 vs. vehicle, $P < 0.0001$; Student t test). Treatment started 4 days post-inoculation. **D,** Individual tumors by group. **E,** Kaplan–Meier plot indicates enhanced survival with IK-175 plus anti-PD-1 over anti-PD-1 alone in CT26 (log-rank Mantel–Cox test).

increase in M1 macrophages leading to an increase M1:M2 ratio, corroborating previous studies indicating the key role of AHR in the tumor immune microenvironment. IK-175 has no effect on human or murine cell line proliferation suggesting it does not directly suppress or enhance tumor cell growth. Rather, the antiproliferative effects of IK-175 are mediated by its ability to stimulate a proinflammatory tumor immune microenvironment.

On-target activity in vivo was demonstrated in mice in a dose-dependent and time-dependent manner in a liver and spleen pharmacodynamic assay. IK-175 only demonstrated AHR antagonistic activity with no activation of AHR in any of the performed experiments. Additionally, IK-175 has antitumor growth activity in syngeneic mouse tumor models and leads to enhanced tumor growth inhibition and survival in combination with the checkpoint inhibitor anti-PD-1 in multiple tumors, including an increased number of CRs. The mice with CRs did not develop tumors when rechallenged with tumor cells, indicating immune memory. The combination activity supports combining IK-175 and checkpoint inhibitors in patients with cancer. This combination has the potential for a better clinical response than single-agent checkpoint inhibitors that have had variable responses in different tumor types. Finally, IK-175 demonstrates combination activity with the chemotherapy liposomal doxorubicin. Chemotherapy treatment that leads to cancer cell death can stimulate the innate immune response (33). This immunogenic cell death elicits an innate response due to induction of Danger Associated Molecular Patterns proteins that, along with tumor-associated antigens, signal DC maturation and antigen presentation to trigger immune activation. We demonstrate activation of AHR in tumors of mice treated with

Downloaded from http://aacrjournals.org/mct/article-pdf/21/8/1261/3182218/1261.pdf by guest on 23 February 2024

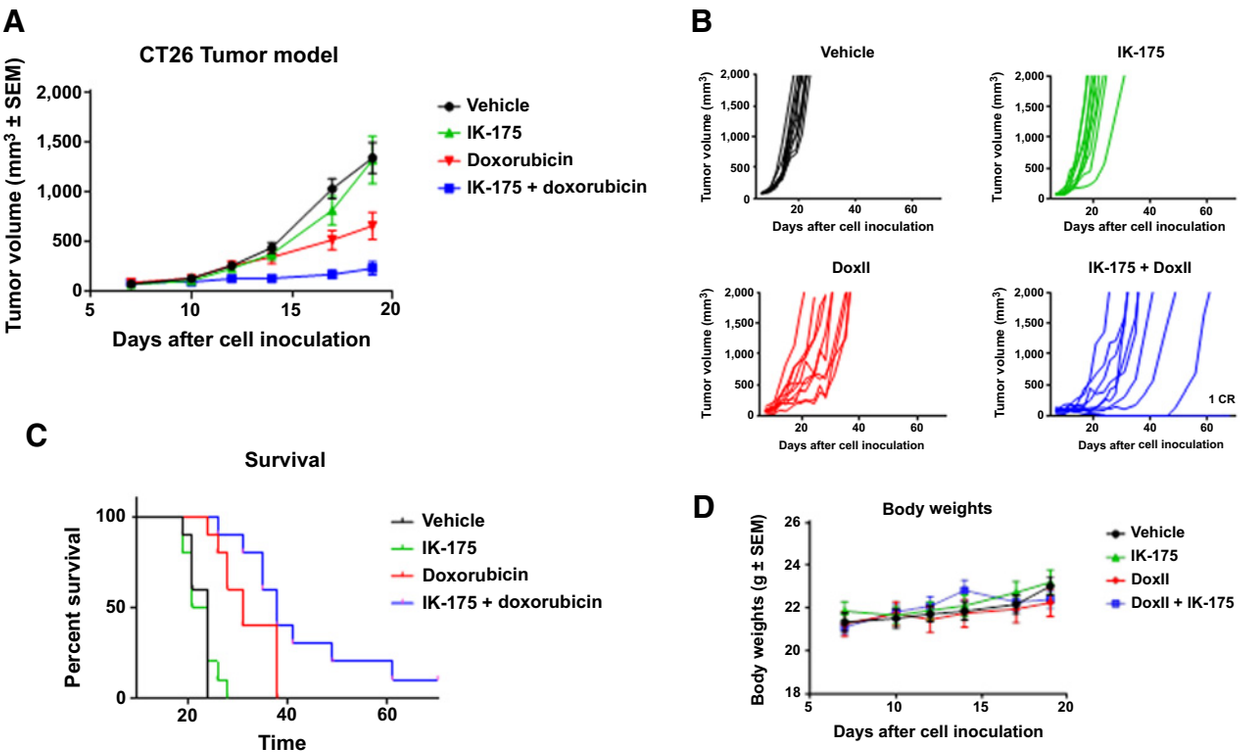

Figure 5.

Combination activity of IK-175 in combination with liposomal doxorubicin on CT26 tumor growth. IK-175 at 25 mg/kg, orally, every day; liposomal doxorubicin at 1 mg/kg, i.v., every 7 days for four doses. **A,** Tumor growth over time in CT26 (liposomal doxorubicin vs. vehicle, $P = 0.0038$; IK-175 plus liposomal doxorubicin vs. vehicle, $P < 0.0001$; IK-175 plus liposomal doxorubicin, $P = 0.0116$, unpaired t test). **B,** Individual tumors by group. **C,** Kaplan–Meier plot indicates enhanced survival with IK-175 + 1 mg/kg liposomal doxorubicin vs. liposomal doxorubicin alone. **D,** Body weights over course of study.

liposomal doxorubicin. In vivo efficacy studies demonstrate synergy when IK-175 is dosed with liposomal doxorubicin. These data suggest that AHR inhibition may combine well with agents that induce AHR activity and/or immunogenic cell death and provide support for exploring additional rational combinations.

Previous reports suggest a tumor suppressor role for AHR (34, 35). These studies showed increased colon tumorigenesis in AHR knockout mice and suggested that this could have been due in part to increased inflammation stimulating tumor formation. The studies suggest an interplay between the β-catenin and AHR pathways in the colon; knock-out of AHR increased tumorigenesis in APC knockout mice and dosing with AHR ligands reduced inflammation and tumor formation (35). AHR is known to function in gut immune homeostasis and dysregulation can have adverse effects including increased colon cancer risk (36). There have been studies reporting that AHR inhibition leads to increased tumor growth, as demonstrated by AHR KO or treatment with the AHR inhibitor CH-22319 in the MC38 model (37). Our studies with IK-175 did not demonstrate enhanced tumor formation or growth in any *in vitro* or *in vivo* models. Similarly, no protumor effects were observed with CH-223191 in our previous studies and tumors implanted into AHR KO mice had growth delays (9). The reason for the discrepancy between these studies on the tumorigenic effects of AHR are not evident, though perhaps can be attributed to differences between mouse models. Regardless, the totality of the IK-175 data support its use to reverse tumor immune suppression in cancer.

Immune suppression plays a major role in tumor aggressiveness and poor patient prognosis. Although approved therapies have made advances in reversing tumor immune suppression leading to improved patient outcome, there is still a great need for better therapies. The role of the IDO1/TDO2/AHR pathway in driving tumor immune suppression is well established (8, 10), and there is a correlation between high pathway activity and poor prognosis in many cancer types. Preclinical studies on the IDO1/TDO2 pathway showed great promise for therapies targeting these enzymes to reduce the immune suppressive metabolite kynurenine. However, initial clinical trials with IDO1 selective inhibitors have not been successful at addressing this potential; some of the less than successful trials were likely partly due to suboptimal dosing (38, 39). In addition, there is ample evidence that kynurenine is produced by TDO2 in multiple cancers and the current IDO1 inhibitors would not have activity in these tumors. The IDO1/TDO2/AHR axis is a promising target if approached with the right therapeutic and strategy, including patient selection. Given that AHR is the receptor for kynurenine and other immune suppressive ligands, it could serve as a better therapeutic target for reversing immune suppression caused by kynurenine and other AHR ligands. Recent in-depth mechanistic studies demonstrate a significant AHR-driven activity in both T cells and myeloid cells of the tumor microenvironment, strongly supporting a role for AHR, especially in tumors with high IDO1, TDO2, and AHR activity (9, 20, 40). We have identified IK-175 as a potent, selective, orally active AHR inhibitor that is

Downloaded from http://aacrjournals.org/mct/article-pdf/21/8/1261/3182218/1261.pdf by guest on 23 February 2024

currently being evaluated in a phase I clinical trial in patients with advanced solid tumors and urothelial carcinoma as a single agent and in combination with the anti-PD-1 antibody nivolumab.

Authors' Disclosures

K. McGovern reports a patent for WO2022/094567 pending. A.C. Castro reports personal fees from Ikena Oncology outside the submitted work; also has a patent for WO2020081636 issued, a patent for WO2021108528 and WO2021108469 pending. J. Cavanaugh reports other support from Ikena Oncology outside the submitted work; and reports employment with Ikena Oncology. M. Walsh reports personal fees from Obsidian Therapeutics and CatamaranBio outside the submitted work. M. Manfredi reports employment with Ikena Oncology and has rights to IK-175. No disclosures were reported by the other authors.

Authors' Contributions

K. McGovern: Conceptualization, supervision, validation, visualization, writing–original draft. **A.C. Castro:** Conceptualization, supervision, validation, investigation, methodology, project administration, writing–review and editing. **J. Cavanaugh:** Conceptualization, formal analysis, validation, investigation, visualization, methodology, writing–review and editing. **S. Coma:** Conceptualization, formal analysis, validation, investigation, methodology. **M. Walsh:** Conceptualization, formal analysis, validation, investigation, methodology. **J. Tchaicha:** Conceptualization, formal analysis, validation, investigation, methodology. **S. Syed:** Conceptualization, formal analysis, investigation, visualization, methodology. **P. Natarajan:** Conceptualization, investigation, visualization, methodology. **M. Manfredi:** Conceptualization, supervision, funding acquisition, validation, project administration. **X.M. Zhang:** Conceptualization, supervision, validation, project administration, writing–review and editing. **J. Ecsedy:** Conceptualization, supervision, validation, project administration, writing–review and editing.

Acknowledgments

This work was funded by Ikena Oncology. We thank Felipe Campesato, Taha Merghoub, and Jedd Wolchok for the B16-IDO1 cell line and for helpful discussions. We are grateful to Gary Perdew for performing the AHR binding assay and Michael Denison for supplying the DRE-Luc reporter plasmid.

Received December 8, 2021; revised April 1, 2022; accepted May 27, 2022; published first June 6, 2022.

References

1. Chen DS, Mellman I. Oncology meets immunology: the cancer-immunity cycle. Immunity 2013;39:1–10.
2. Finn OJ. Immuno-oncology: understanding the function and dysfunction of the immune system in cancer. Ann Oncol 2012;23 Suppl 8:viii6–9.
3. Rothhammer V, Quintana FJ. The aryl hydrocarbon receptor: an environmental sensor integrating immune responses in health and disease. Nat Rev Immunol 2019;19:184–97.
4. Shinde R, McGaha TL. The aryl hydrocarbon receptor: connecting immunity to the microenvironment. Trends Immunol 2018;39:1005–20.
5. Stevens EA, Mezrich JD, Bradfield CA. The aryl hydrocarbon receptor: a perspective on potential roles in the immune system. Immunology 2009;127:299–311.
6. Ala M. The footprint of kynurenine pathway in every cancer: a new target for chemotherapy. Eur J Pharmacol 2021;896:173921.
7. Liu XH, Zhai XY. Role of tryptophan metabolism in cancers and therapeutic implications. Biochimie 2021;182:131–9.
8. Wang Z, Snyder M, Kenison JE, Yang K, Lara B, Lydell E, et al. How the AHR became important in cancer: the role of chronically active AHR in cancer aggression. Int J Mol Sci 2020;22:387.
9. Campesato LF, Budhu S, Tchaicha J, Weng CH, Gigoux M, Cohen IJ, et al. Blockade of the AHR restricts a Treg-macrophage suppressive axis induced by L-Kynurenine. Nat Commun 2020;11:4011.
10. Gargaro M, Manni G, Scalisi G, Puccetti P, Fallarino F. Tryptophan metabolites at the crossroad of immune-cell interaction via the aryl hydrocarbon receptor: implications for tumor immunotherapy. Int J Mol Sci 2021;22:4644.
11. Opitz CA, Litzenburger UM, Sahm F, Ott M, Tritschler I, Trump S, et al. An endogenous tumour-promoting ligand of the human aryl hydrocarbon receptor. Nature 2011;478:197–203.
12. Funatake CJ, Marshall NB, Steppan LB, Mourich DV, Kerkvliet NI. Cutting edge: activation of the aryl hydrocarbon receptor by 2,3,7,8-tetrachlorodibenzo-p-dioxin generates a population of CD4+ CD25+ cells with characteristics of regulatory T cells. J Immunol 2005;175:4184–8.
13. Quintana FJ, Basso AS, Iglesias AH, Korn T, Farez MF, Bettelli E, et al. Control of T(reg) and T(H)17 cell differentiation by the aryl hydrocarbon receptor. Nature 2008;453:65–71.
14. Gutierrez-Vazquez C, Quintana FJ. Regulation of the immune response by the aryl hydrocarbon receptor. Immunity 2018;48:19–33.
15. Zhou L. AHR function in lymphocytes: emerging concepts. Trends Immunol 2016;37:17–31.
16. Liu Y, Liang X, Dong W, Fang Y, Lv J, Zhang T, et al. Tumor-repopulating cells induce PD-1 expression in CD8(+) T cells by transferring kynurenine and AhR activation. Cancer Cell 2018;33:480–94.
17. Takenaka MC, Gabriely G, Rothhammer V, Mascanfroni ID, Wheeler MA, Chao CC, et al. Control of tumor-associated macrophages and T cells in glioblastoma via AHR and CD39. Nat Neurosci 2019;22:729–40.
18. Murray IA, Patterson AD, Perdew GH. Aryl hydrocarbon receptor ligands in cancer: friend and foe. Nat Rev Cancer 2014;14:801–14.
19. Xue P, Fu J, Zhou Y. The aryl hydrocarbon receptor and tumor immunity. Front Immunol 2018;9:286.
20. Kenison JE, Wang Z, Yang K, Snyder M, Quintana FJ, Sherr DH. The aryl hydrocarbon receptor suppresses immunity to oral squamous cell carcinoma through immune checkpoint regulation. Proc Natl Acad Sci U S A 2021;118:e2012692118.
21. Boitano AE, Wang J, Romeo R, Bouchez LC, Parker AE, Sutton SE, et al. Aryl hydrocarbon receptor antagonists promote the expansion of human hematopoietic stem cells. Science 2010;329:1345–8.
22. Fang ZZ, Krausz KW, Nagaoka K, Tanaka N, Gowda K, Amin SG, et al. In vivo effects of the pure aryl hydrocarbon receptor antagonist GNF-351 after oral administration are limited to the gastrointestinal tract. Br J Pharmacol 2014;171:1735–46.
23. Rouse M, Singh NP, Nagarkatti PS, Nagarkatti M. Indoles mitigate the development of experimental autoimmune encephalomyelitis by induction of reciprocal differentiation of regulatory T cells and Th17 cells. Br J Pharmacol 2013;169:1305–21.
24. Castro AC, inventor; Kyn Therapeutics, assignee. Indole AHR inhibitors and uses thereof. United States patent 10,570,138. Feb 25, 2020.
25. Han D, Nagy SR, Denison MS. Comparison of recombinant cell bioassays for the detection of Ah receptor agonists. Biofactors 2004;20:11–22.
26. Poland A, Glover E, Ebetino FH., Kende AS. Photoaffinity labeling of the Ah receptor. J Biol Chem 1986;261:6352–65.
27. Flaveny CA, Murray IA, Chiaro CR, Perdew GH. Ligand selectivity and gene regulation by the human aryl hydrocarbon receptor in transgenic mice. Mol Pharmacol 2009;75:1412–20.
28. Lawrence BP, Denison MS, Novak H, Vorderstrasse BA, Harrer N, Neruda W, et al. Activation of the aryl hydrocarbon receptor is essential for mediating the anti-inflammatory effects of a novel low-molecular-weight compound. Blood 2008;112:1158–65.
29. Soshilov AA, Denison MS. Ligand promiscuity of aryl hydrocarbon receptor agonists and antagonists revealed by site-directed mutagenesis. Mol Cell Biol 2014;34:1707–19.
30. Kim SH, Henry EC, Kim DK, Kim YH, Shin KJ, Han MS, et al. Novel compound 2-methyl-2H-pyrazole-3-carboxylic acid (2-methyl-4-o-tolylazo-phenyl)-amide (CH-223191) prevents 2,3,7,8-TCDD-induced toxicity by antagonizing the aryl hydrocarbon receptor. Mol Pharmacol 2006;69:1871–8.
31. Holmgaard RB, Zamarin D, Li Y, Gasmi B, Munn DH, Allison JP, et al. Tumor-expressed IDO recruits and activates MDSCs in a Treg-dependent manner. Cell Rep 2015;13:412–24.
32. Gilbert LA, Hemann MT. DNA damage-mediated induction of a chemoresistant niche. Cell 2010;143:355–66.

Downloaded from http://aacrjournals.org/mct/article-pdf/21/8/1261/3182218/1261.pdf by guest on 23 February 2024

33. Gotwals P, Cameron S, Cipolletta D, Cremasco V, Crystal A, Hewes B, et al. Prospects for combining targeted and conventional cancer therapy with immunotherapy. Nat Rev Cancer 2017;17:286–301.
34. Ikuta T, Kobayashi Y, Kitazawa M, Shiizaki K, Itano N, Noda T, et al. ASC-associated inflammation promotes cecal tumorigenesis in aryl hydrocarbon receptor-deficient mice. Carcinogenesis 2013;34: 1620–7.
35. Kawajiri K, Kobayashi Y, Ohtake F, Ikuta T, Matsushima Y, Mimura J, et al. Aryl hydrocarbon receptor suppresses intestinal carcinogenesis in ApcMin/+ mice with natural ligands. Proc Natl Acad Sci U S A 2009;106: 13481–6.
36. Rannug A. How the AHR became important in intestinal homeostasis-a diurnal FICZ/AHR/CYP1A1 feedback controls both immunity and immunopathology. Int J Mol Sci 2020;21:5681.
37. Yakkundi P, Gonsalves E, Galou-Lameyer M, Selby MJ, Chan WK. Aryl hydrocarbon receptor acts as a tumor suppressor in a syngeneic MC38 colon carcinoma tumor model. Hypoxia (Auckl) 2019;7:1–16.
38. Smith M, Newton R, Owens S, Gong X, Tian C, Maleski J, et al., editors. Retrospective pooled analysis of epacadostat clinical studies identifies doses required for maximal pharmacodynamic effect in anti-PD-1 combination studies. Poster presented at the Society for Immunotherapy of Cancer (SITC) 35th Anniversary Annual Meeting; November 11–14, 2020; Virtual.
39. Van den Eynde BJ, van Baren N, Baurain J-F. Is there a clinical future for IDO1 inhibitors after the failure of epacadostat in melanoma? Annu Rev Cancer Biol 2020;4:241–56.
40. Leclerc D, Staats Pires AC, Guillemin GJ, Gilot D. Detrimental activation of AhR pathway in cancer: an overview of therapeutic strategies. Curr Opin Immunol 2021;70:15–26.

Downloaded from http://aacrjournals.org/mct/article-pdf/21/8/1261/3182218/1261.pdf by guest on 23 February 2024